

**Shutting down or  
powering up a (U)LIRG?  
Merger components in  
distinctly different  
evolutionary states in  
IRAS 19115-2124 (The Bird)**

Vaisanen et al. 2017

MNRAS.471.2059V

arXiv: 1701.00890

Presenter: K. Kushibiki

# Contents

Abstract

1. Introduction

2. Observation and Data Reductions

3. Results

4. Discussion

5. Bird at High-redshift

# Abstract

SINFONI near-infrared IFU spectroscopy and SALT optical long-slit spectroscopy

→ **History of nearby merging luminous infrared galaxy** “The Bird”(IRAS19115-2114)

- SINFONI NIR IFU → line-ratio maps
- SALT optical spectra → stellar population fitting

The distinct component separate in line-ratio diagnostic

- Off-nuclear starburst: 60-70% of total SFR, 4-7 Myr age, constant long-term SF
- Most massive nucleus: quenched with a starburst age > 40 Myr, budding AGN
- Secondary massive nucleus: intermediate stage
  - Latter two have old population consistent with starburst triggered > 1 Gyr ago

→ Simplest explanation of the history is **a triple merger**

The Bird offers an opportunity to **witness multiple stages**

- triggering and quenching of SF
- the early appearance of AGN activity

And cautionary note on interpretations of high-redshift observation with low spatial resolution and without infrared data

# 1. Introduction

The strongest starburst activity is linked to interactions or merger: ULIRGs

- Inflow of gas → nuclear starburst in dusty environment
- Strong winds, growing BH and following AGN → terminate starburst

Not all ULIRGs fit to the above scenario

- Strongest starburst in overlap region (Mirabel+1998, Karl+2010)
- Off-nuclear starburst (e.g. Jarret+2006, Herrero-Illana+2017)
- Multiple interactions

In this paper, a case of a LIRG system ( $\log L_{IR}/L_{\odot} = 11.9$ ); "The Bird"

NIR IFU data and optical spectra

→ spatial and velocity-based disentangling of line emissions, which is important for complex target such as LIRGs

Key points: "composite objects" for many advanced mergers

- Mixture of AGN and SF emission
- Shock emission together with SF

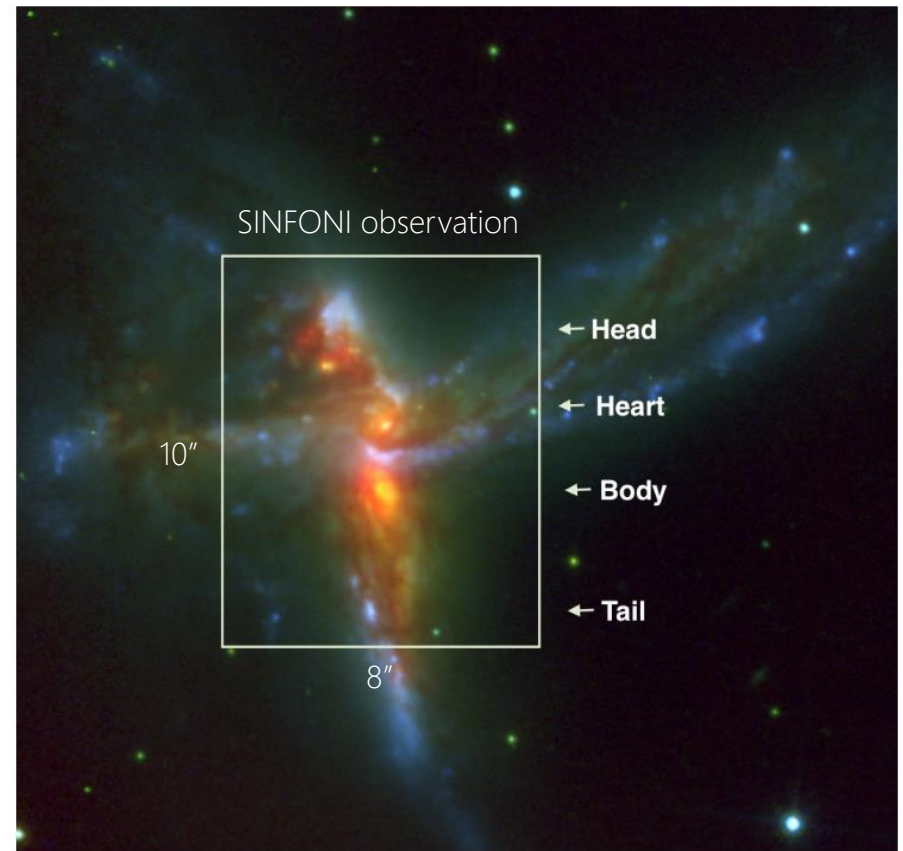
What is the case for the Bird ? ANG or shock with SF or only shock ?

# 1. Introduction

## 1.1 IRAS19115-2124: the Bird

- Distance = 200 Mpc ( $z \sim 0.05$ )
- Infrared luminosity:  $\log L_{IR}/L_{\odot} = 11.9$
- Far-IR SED based SFR  $\sim 190 M_{\odot}/\text{yr}$
- Two main nuclei (Heart and Body)
  - $\sim 1.5$  kpc ( $1.5''$ ) projected distance
  - Both have bars
- 20 kpc scale tidal tail
- Third component: satellite galaxy (Head)
  - projected 2 kpc North of two nuclei

Fig. 1. K-band AO image + HST/I, B



# 2. Observation and data reduction

## 2.1. SINFONI

### **Observation: Near infrared IFU data**

- K-band (1.95-2.45 $\mu$ m, R~4000): final FOV=9.5"x10.5", pixel scale=0".125, total 3600s
- J-band (1.10-1.40 $\mu$ m, R~2000): the same manner as K-band, total 1800s
- Higher resolution K-band:  
3"x3" area centered in between the Heart and Head, total 3600s  
Natural guide star AO: FWHM = 0.4" (Seeing: 0.6"-0.9")

### **Date reduction: ESOREX (Freudling+2013)**

- Dark, flat, detector linearity, geometric distortion corrections
- Wavelength calibrations using Neon and Argon arcs
- Telluric correction and initial flux calibration with spectrophotometric standards  
→ Final flux calibration with photometry of Vaisanen+2008(K-band), 2MASS (J-band)  
Absolutely accurate within 20%

# 2. Observation and data reduction

## 2.2 SALT

### Observation: 2 optical spectra

- R~1000
- From blue-ward of [OII] $\lambda$ 3727 to 7500 AA
- Total 1200s (first set) and 1800s (second set)
- PA=10 going through the Head and Body+Tail (Just to the east of Heart nucleus)

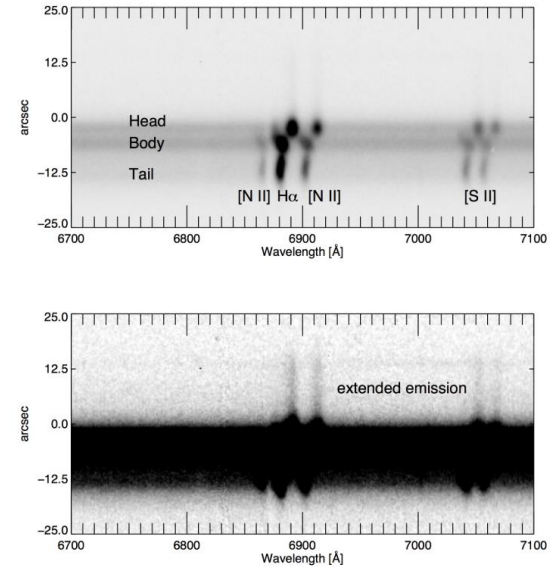
### Reduction: PySALT (Crawford+2010)

- 4 apertures: Head, Tail, Body+Heart, North of Head (~1.6" seeing limited constraint)
- 2 spectra were averaged per galaxy component and aperture

## 2.2 VISIR

- Mid-infrared NB imaging for the PAH emission distribution
- 0.8" seeing condition, total 1800s
- Reduction with ESOREX
- S/N is not enough for a detailed study, but general features are recognizable

Fig. 2 Salt spectrum



# 3. Results

## 3.1. Analysis of the IFU data

QFitsView program

- Continuum subtracted line maps
- Aperture for each component are shown in Fig 3
- Velocity fields using strong emission lines

## 3.2. Emission features

$P\alpha$ : Ionizing OB-star population of  $\sim 10$  Myr or less

[FeII]: Shocking from SN remnants  $\rightarrow$  older  $\sim 30$  Myr

HeI: Youngest stellar population

$H_2 1-0S(1)$  (Strongest in  $H_2$  emissions): Warm molecular gas

Emission line fluxes

- IDL aperture photometry of emission feature maps
  - From spectra extracted from spatial apertures in the datacubes
- $\rightarrow$  Line ratios (Memo: Calzetti reddening law)

Fig. 3. collapsed K-band

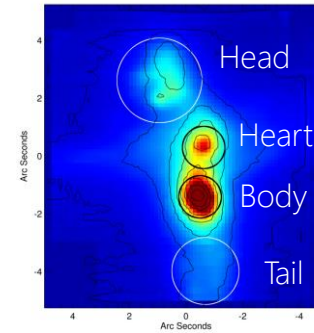
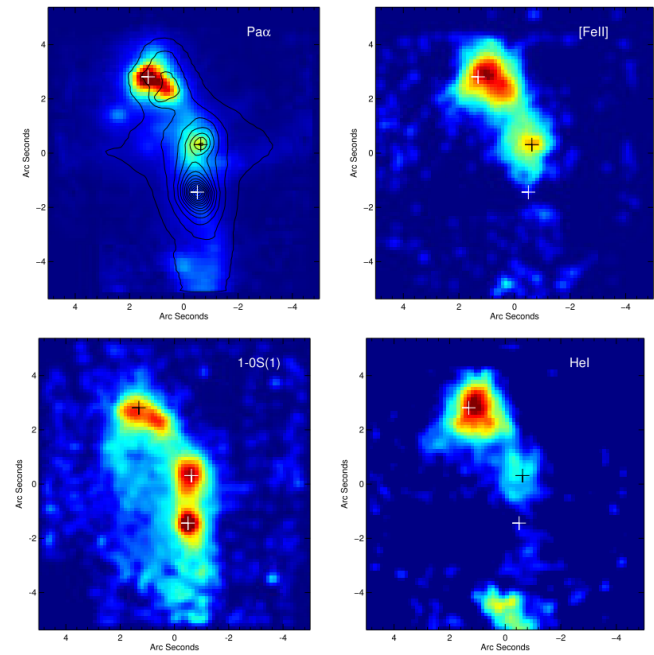


Table 1

Aperture	Radius [arcsec and kpc]
Body	0.75
Body-nuc	0.25
Heart	0.75
Heart-nuc	0.25
Head	1.50
Tail	1.25

\*  $1'' \sim 1$  kpc @  $z \sim 0.05$

Fig. 4. emission maps



# 3. Results (Spectra)

Fig. 5. J-band spectra

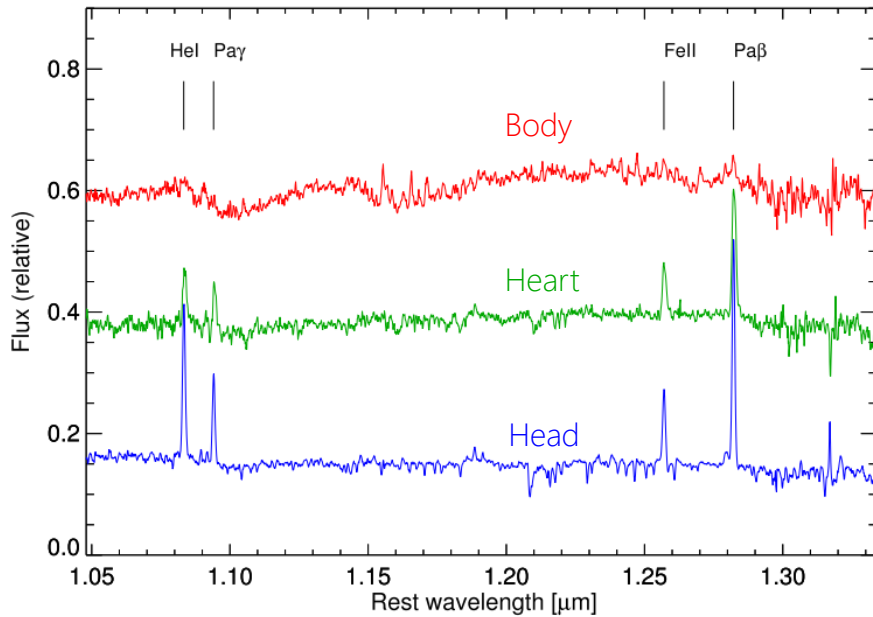
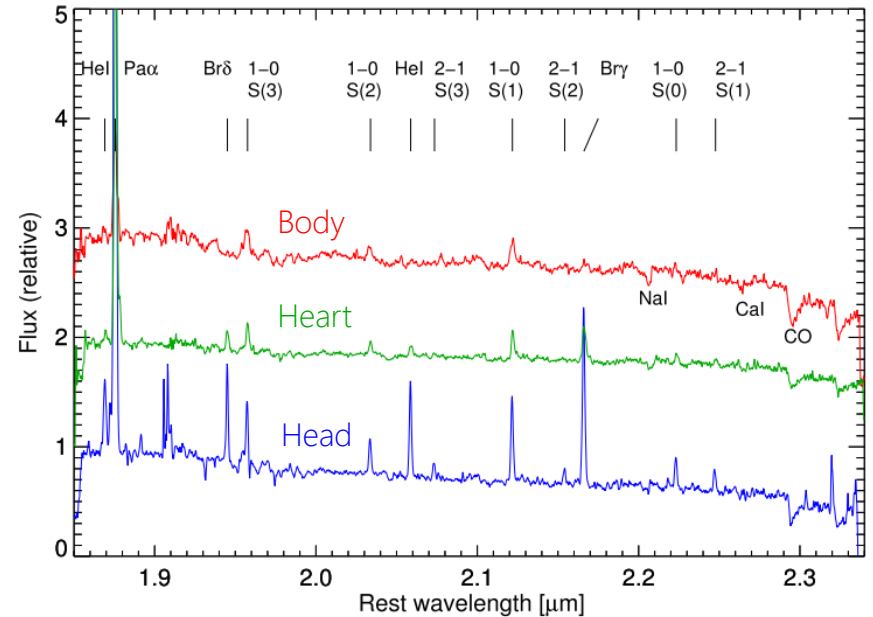


Fig. 5. K-band spectra



# 3. Results (Tables)

Regions aperture		Body 0.75	Body-nuc 0.25	Heart 0.75	Heart-nuc-nuc 0.25	Head 1.5	Tail 1.25	Integ. full
Line	$\lambda_0$ [ $\mu\text{m}$ ]							
HeI(J)	1.0833	5.77 ± 2.02	0.73 ± 0.71	13.46 ± 3.09	1.71 ± 1.10	70.60 ± 7.06	27.54 ± 4.41	212.72 ± 12.26
Pa $\gamma$	1.0941	4.72 ± 2.39	0.56 ± 0.82	9.15 ± 2.75	1.24 ± 0.94	34.24 ± 5.97	12.60 ± 3.81	114.12 ± 11.84
FeII	1.2570	2.38 ± 1.27	0.26 ± 0.42	9.51 ± 2.55	1.47 ± 1.00	37.87 ± 5.09	6.06 ± 2.04	110.79 ± 8.71
Pa $\beta$	1.2822	10.13 ± 2.41	1.69 ± 0.83	24.13 ± 3.96	3.64 ± 1.53	96.75 ± 8.02	26.42 ± 4.17	248.82 ± 13.06
Pa $\alpha$	1.8756	55.45 ± 4.43	6.44 ± 1.51	127.95 ± 6.74	20.92 ± 2.72	495.55 ± 13.26	135.78 ± 6.94	1286.40 ± 21.36
Br $\delta$	1.9451	1.66 ± 1.05	0.26 ± 0.33	4.98 ± 1.22	0.82 ± 0.49	28.10 ± 2.89	6.95 ± 1.44	49.64 ± 3.84
1-0S(3)	1.9576	16.42 ± 2.25	2.91 ± 0.95	11.76 ± 1.92	1.76 ± 0.78	22.47 ± 2.85	10.27 ± 1.86	142.52 ± 6.89
1-0S(2)	2.0338	3.95 ± 0.98	0.79 ± 0.42	3.98 ± 1.19	0.74 ± 0.49	9.36 ± 1.77	4.56 ± 1.08	41.91 ± 3.73
HeI(K)	2.0587	1.35 ± 0.69	0.04 ± 0.13	3.57 ± 1.12	0.57 ± 0.45	23.25 ± 2.87	5.25 ± 1.36	45.32 ± 4.01
2-1S(3)	2.0735	0.00 ± 0.00	0.00 ± 0.00	0.00 ± 0.00	0.00 ± 0.00	1.91 ± 0.17	0.00 ± 0.00	0.00 ± 0.00
1-0S(1)	2.1218	10.04 ± 1.86	1.88 ± 0.83	10.18 ± 1.87	1.51 ± 0.74	23.20 ± 2.85	10.82 ± 1.96	109.78 ± 6.24
2-1S(2)	2.1542	0.00 ± 0.00	0.00 ± 0.00	0.00 ± 0.00	0.00 ± 0.00	1.80 ± 0.20	0.00 ± 0.00	0.00 ± 0.00
Br $\gamma$	2.1661	7.22 ± 1.68	0.91 ± 0.59	13.92 ± 2.33	2.38 ± 0.96	54.57 ± 4.61	14.04 ± 2.34	142.93 ± 7.46
1-0S(0)	2.2233	3.17 ± 1.14	0.58 ± 0.52	3.51 ± 1.09	0.49 ± 0.39	10.91 ± 2.15	4.35 ± 1.28	48.32 ± 4.31
2-1S(1)	2.2477	4.82 ± 1.27	0.66 ± 0.50	3.42 ± 1.01	0.40 ± 0.36	7.55 ± 1.56	3.47 ± 0.99	41.94 ± 3.63

**Table 2.** Observed line fluxes, in units of  $10^{-16} \text{ erg s}^{-1} \text{ cm}^{-2}$ . Zero values mark non-detections. Aperture size is in units of kpc (and arcsec).

Region	Body	Body-nuc	Heart	Heart-nuc	Head	Tail	Integ.
FeII / Pa $\beta$	0.23	0.15	0.39	0.40	0.39	0.23	0.45
1-0 S(1) / Br $\gamma$	1.39	2.07	0.73	0.63	0.43	0.77	0.77
1-0 S(1) / Pa $\alpha$	0.18	0.29	0.08	0.07	0.05	0.08	0.09
FeII / 1-0 S(1)	0.24	0.14	0.93	0.97	1.63	0.56	1.01
HeI / 1-0 S(1)	0.13	0.02	0.35	0.38	1.00	0.49	0.41
1-0 S(0) / 1-0 S(1)	0.32	0.31	0.34	0.32	0.47	0.40	0.44
1-0 S(2) / 1-0 S(1)	0.39	0.42	0.39	0.49	0.40	0.42	0.38
1-0 S(2) / 1-0 S(0)	1.25	1.36	1.13	1.51	0.86	1.05	0.87
1-0 S(3) / 1-0 S(1)	1.64	1.55	1.16	1.17	0.97	0.95	1.30
2-1 S(1) / 1-0 S(1)	0.48	0.35	0.34	0.26	0.33	0.32	0.38
HeI / Br $\gamma$	0.29	0.07	0.39	0.46	0.68	0.42	0.40
$A_V$ (Pa $\beta$ /Pa $\gamma$ )	2.1	6.2	4.6	5.9	5.4	1.8	2.3
$A_V$ (Pa $\alpha$ /Pa $\beta$ )	6.4	4.0	6.2	6.7	6.0	6.0	6.0
$A_V$ (Br $\gamma$ /Pa $\alpha$ )	10.2	12.0	6.1	7.1	6.4	5.0	6.6
$A_V$ (Br $\gamma$ /Br $\delta$ ) [weak]	32.3	25.6	18.7	19.9	7.5	8.7	19.6

**Table 3.** Column densities and line ratios. Note that the ratios are not extinction corrected in the table, though all figures and maps showing line ratios are corrected for extinction adopting the values using the Br $\gamma$ /Pa $\alpha$  derived  $A_V$ .

# 3. Results

## 3.3. Kinematics and Masses

### Radial velocities and velocity dispersion

#### Gas

NIR emission and H $\alpha$  has consistent value except for the Body

← Deeper component probed by the SINFONI data

#### CO-band-head absorption region

→ Kinematics of stellar component

Fitting with stellar giant and supergiant template

→ Good with type K5III to M0III (M0I)

#### Comparison of above two

Gas  $\sigma$  > Stellar  $\sigma$

→ Complex velocity structures and flows

Table 4

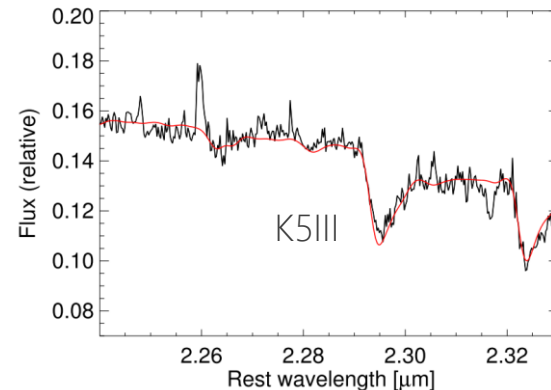
	Body-nuc	Heart-nuc	Head	Tail
		$v_r$ [km/s]		
Pa $\alpha$	14750 <sup>1</sup>	14470 <sup>1</sup>	14940	14550
H <sub>2</sub> 1-0 S(1)	14780 <sup>1</sup>	14500 <sup>1</sup>	14920	14540
CO band	14780	14540	15000	14550
H $\alpha$	14590 <sup>2</sup>	14520 <sup>2</sup>	14940	14470
		$\sigma$ [km/s]		
Pa $\alpha$	180	140	100	90
1-0(S1)	220	120	100	90
CO band	150	130	120 <sup>3</sup>	70
		$v_{rot}$ [km/s]		
Pa $\alpha$	170	270	100	–
		$m_{dyn}$ [ $10^{10} M_{\odot}$ ]		
	10	7	2	–

<sup>1</sup> Multiple velocity components, strongest one adopted.

<sup>2</sup> From V08.

<sup>3</sup> A small 375 kpc radius area in the Head.

Fig. 6. CO-band-head of Body-nuc



# 3. Results

## 3.3. Kinematics and Masses

### Full Velocity maps

- Horizontally rotating Heart
- Head disjoint from the Heart in the West, but smoother transition over the East wing
- Disk rotation in the Body location  
→ Not detected in previous optical obs.

	Body	Heart	Head
$v_{\text{rot}}$	170 km/s	270 km/s	100 km/s

### Dynamical mass from $\sigma$ and rotation

- Body ( $\sigma=140\text{km/s}$ ,  $r_e=2.4\text{kpc}$ )  
→  $\sim 1 \times 10^{11} M_{\odot}$  ( $> V08$  optical ionized gas)
  - Heart ( $\sigma=130\text{km/s}$ ,  $r_e=1.3\text{kpc}$ )  
→  $\sim 7 \times 10^{10} M_{\odot}$  ( $\sim V08$ )
  - Head using smaller aperture than default ( $\sigma=70-90$ ,  $r_e=0.8\text{kpc}$ )  
→  $\sim 2 \times 10^{10} M_{\odot}$
- Progenitors are  $1-2 \times 10^{11} M_{\odot}$  massive disks

Fig. 7. velocity maps

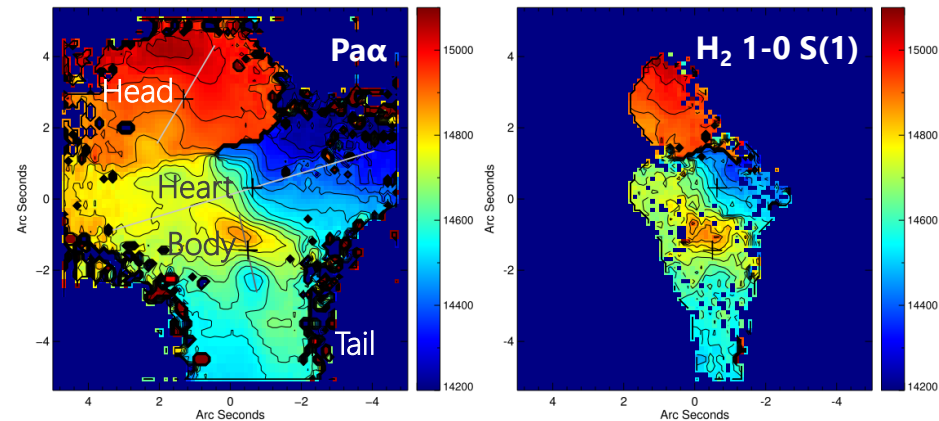
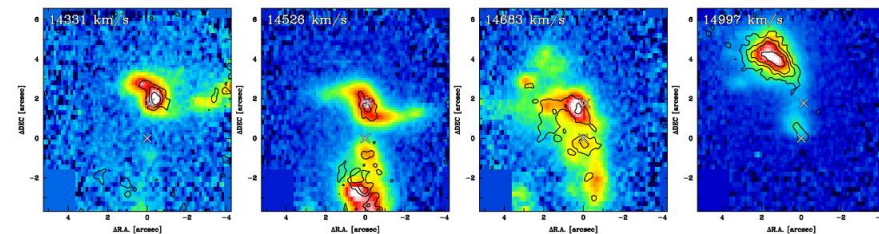


Fig. 8 velocity slices of Paα map



\*V08: Vaisanen+2008 observing the Bird using SALT and VLT/NACO

# 3. Results

## 3.4. Stellar populations and metallicities

### Optical spectrum fitting with STARLIGHT (Cid Fernandes+2015)

BC03 SSP & Padova track

Head, Body+Heart, Tail, North of Head

→ Light-weighted mean Age: 0.9-2.4 Gyr

Mass-weighted mean Age: 10 Gyr

Indicative SFH: SSP fraction (Fig. 10)

→ Body+Heart has a significant peak at 1 Gyr

↔ Others have more extended distribution

Tail & Extended have population age

~100Myr-1Gyr where Body+Heart devoid of SF

Stellar [Fe/H] metallicity: Head has lower stellar metallicity than others

Strong emission line ratios

- Nebular abundance: Uniform over all the apertures  $12 + \log([\text{O}/\text{H}]) \sim 8.8 \pm 0.1$  (Average of O3N2, DO2, N2)  
Just below the mass-metallicity relation

- Line ration: Typical to HII region except for the Extended where  $[\text{NII}]/\text{H}\alpha$ ,  $[\text{SII}]/\text{H}\alpha \sim 0.6$ , shock

Fig. 9. SALT spec.

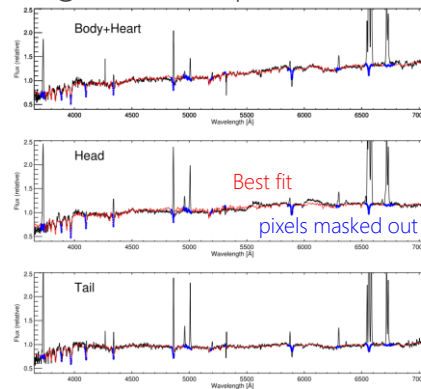


Fig. 10. SSP fraction

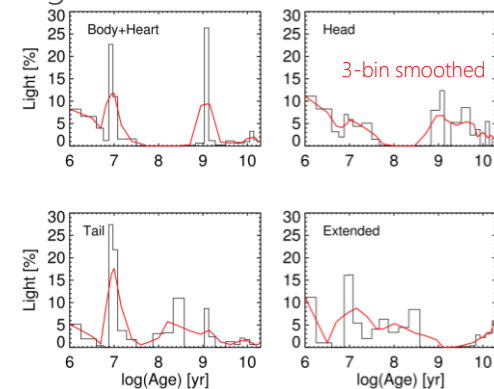


Table 5

	$\text{age}_{\text{light}}^a$ (Myr)	$Z$	$A_V$ (stars) (mag)	< 15Myr (% light)	15 – 800Myr (% light)	800 – 1400Myr (% light)	O/H	$A_V$ (gas) (mag)
Body+Heart	1300 / 60	0.016	1.6	55	2	27	8.78	3.0
Head	2300 / 146	0.011	1.1	42	7	20	8.79	2.5
Tail	900 / 44	0.019	1.5	60	19	9	8.74	2.4
Extended	2400 / 45	0.018	1.2	50	29	0	8.85	1.2

<sup>a</sup> First value is the average in linear space, the second in log space.

# 3. Results

## 3.4. Stellar populations and metallicities

### *A<sub>V</sub> extinction*

- $A_V(\text{stars})=1.1-1.6 \text{ mag} \leftrightarrow A_V(\text{gas})=2.4-3.0 \text{ mag}$  except for the Extended
- Typical in SF regions and lower than NIR derived value

### *NIR absorption lines for further constraints on stellar populations*

Al I, Si I, Ca I absorptions with the model of Maraston2005 discussed in Riffel+2008

- Body & Heart have similar value  $\rightarrow 1 \text{ Gyr}$
  - Tail: Weaker absorption but still detectable with  $EW \sim 1-2 \text{ \AA} \rightarrow 10, 1000 \text{ Myr} ?$
  - Head: Marginally detectable  $EW < 0.7 \text{ \AA}$  but CO is as strong as elsewhere  $\rightarrow 10 \text{ Myr}$
- $\rightarrow$  Head has different history  
and Head-peak without absorption feature have extremely young starburst

Table 6

	CO 2.30 $\mu\text{m}$	Al I 1.13 $\mu\text{m}$	Si I 1.21 $\mu\text{m}$	Ca I 2.27 $\mu\text{m}$	Pa $\alpha$	Br $\gamma$	SB age [Myr]	SP age [Myr]
Body-nuc	19	1.2	2	1.5	14	< 2	40	1000
Heart-nuc	18	1.2	3	2.5	85	13	8	1000
Head	13	< 0.6	–	< 0.5	220	31	6–7	10
Head-peak	< 7	–	–	–	720	105	4	< 9
Tail	16	1.3	< 1	< 1	95	14	8	10, 1000

# 4. Discussion

*Puzzling feature: Lack of very strong star formation in the main nuclei (Body)*

→ Whether a starburst has not even started in the Body or it has been quenched and why?

What are the differences between the Bird components?

What are their evolutionary phase?

## 4.1. Excitation mechanisms

H2 line ratio → thermal and non-thermal process, excitation temperature, thermal heating mechanisms

$$T_{vib} \sim 5600 / \ln(1.355 \times I_{1-0S(1)} / I_{2-1S(1)}) \quad T_{rot} \sim -1113 / \ln(0.323 \times I_{1-0S(2)} / I_{1-0S(0)})$$

$$f_{o/p} = \frac{1.1102 [S(3)/S(1)]^{0.449}}{S(2)/S(1)} 10^{-0.004 A_K} \quad (\text{Reunanen+2002, 2007})$$

The difference between  $T_{vib}$  and  $T_{rot}$  → non-thermal processes

$1-0S(2)/1-0S(0)$ ,  $1-0S(3)/1-S(1)$ , and  $T_{rot}$  show the dominant mechanism (Mouri1994)

- Head & Tail: low  $T_{rot}$  → UV photon (PDR)
- Body & Heart: higher  $T_{rot}$  → shock heating

Fig. 1 from Mouri1994

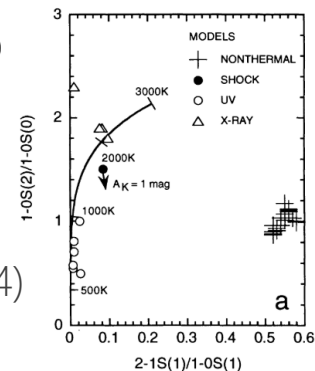


Table 7

Region	Body	Body-nuc	Heart	Heart-nuc	Head	Tail
$T_{vib}$ [K]	4900	3800	3900	3200	3800	3700
$T_{rot}$ [K]	1700	2100	1300	2000	980	1200
$o/p$	3.5	3.2	3.0	2.4	2.7	2.6
Notes:	firscs.	shocks	shocks	shocks	UV	UV

# 4. Discussion

## 4.1. Excitation mechanisms

### Deblending velocity component in the Body

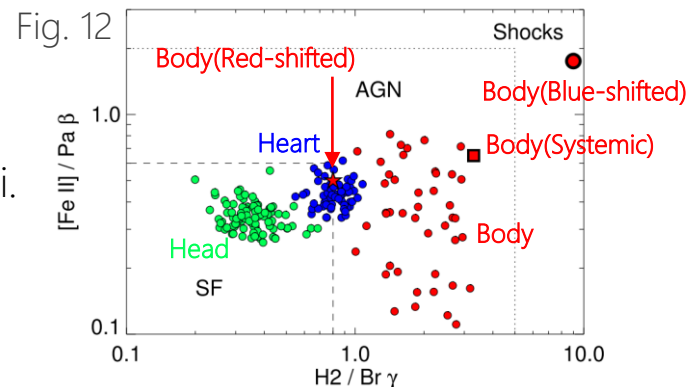
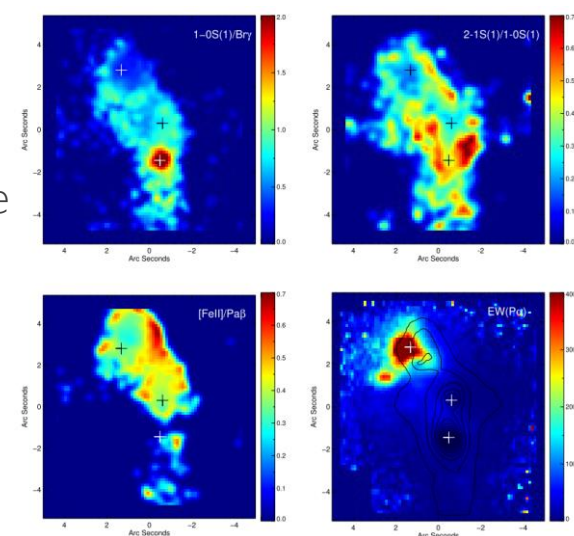
- Largest 2-1S(1)/1-0S(1) and 1-0S(2)/1-0S(0) from *blue-shifted line emission*
- Ratios, temp. of systemic velocity component  $\lesssim$  previous page
- Line ratio of blue-shifted component: UV fluorescence  
Thermal temperature: shock heating
- High 2-1S(1)/1-0S(1) perpendicular the Body disk  
→ Related to conical outflow from nucleus

Summary: Both thermal and non-thermal in the Bird

### 4.1.1. Diagnostic diagram

- Head: young star-forming, photo-ionization
  - Heart: boundary of the SF and AGN
    - nuclear position on the SF side
    - Surrounding area on the AGN side
  - Body: Different between velocity-components
    - Remain in AGN region, but no other AGN signs
- } Shock contami.

Fig. 11. Line ratio maps



# 4. Discussion

## 4.2. Is there an AGN hidden in the Bird?

Previous studies about AGN of the Bird (Mainly results are that there is no AGN)

→ But these observe the Birds as a single object

The simplest explanation from NIR diagnostic: "There is budding AGN at the Body nucleus"

CO-based  $\sigma \rightarrow M_{\text{BH}} \sim 10^{7.6} M_{\odot}$ , with X-ray non-detection with BAT → sub-Eddington level

## 4.3. Age of recent star-formation in the Bird

SF age from H2/Bry, Bry line EW, and "Bry line EW vs CO-index(CO2.3um EW)" (Puxley+1997)

- Head: SB age is consistent with SP age obtained from absorption (~6-7 Myr)
- Tail & Heart: SB age (~8 Myr) smaller than SP age (1 Gyr)
- Body: Non-existence of recombination emissions and [FeII] → lower limit 40 Myr (SNe would happen about 40 Myr until all  $>8M_{\odot}$  stars have gone)  
→ Delay between a starburst and AGN → interesting test of models of early AGN

Table 6

	CO 2.30 $\mu\text{m}$	Al I 1.13 $\mu\text{m}$	Si I 1.21 $\mu\text{m}$	Ca I 2.27 $\mu\text{m}$	Pa $\alpha$	Br $\gamma$	SB age [Myr]	SP age [Myr]
Body-nuc	19	1.2	2	1.5	14	< 2	40	1000
Heart-nuc	18	1.2	3	2.5	85	13	8	1000
Head	13	< 0.6	–	< 0.5	220	31	6–7	10
Head-peak	< 7	–	–	–	720	105	4	< 9
Tail	16	1.3	< 1	< 1	95	14	8	10, 1000

# 4. Discussion

## 4.3 Age of recent star-formation in the Bird

### PAH emission (11.3 $\mu$ m) from VISIR data (Fig. 13)

- Strongest emission from Heart
- PAH appears to avoid the strong SF regions
  - ← Destruction or dilution of PAH carriers
- Condition for PAH destruction or dilution happen at starburst age < 7 Myr

### Narrow velocity slices of Pa $\alpha$ emission

- Several point-like knots in the Heart and Head
- Young super star cluster or young massive cluster
- K-band AO imaging: Point-like sources concentrate on the side facing the larger galaxies
- Triggering massive clusters by compressions of gas

Fig. 13. PAH emission

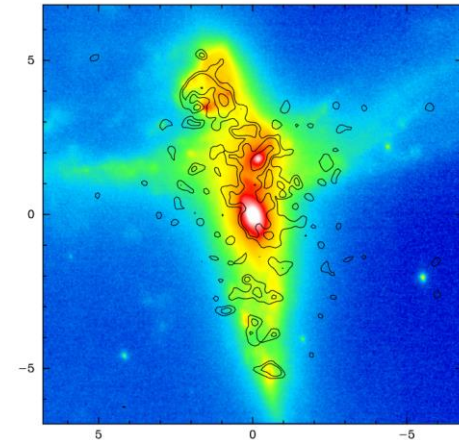
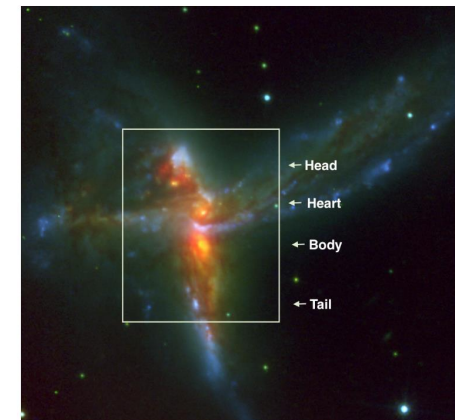


Fig. 1. K-band AO+HST/I, B



# 4. Discussion

## 4.4 Histories of the Bird components

*Different SFH in the regions:* Body+Heart (Bimodal peak) vs Head&Tail (Evenly distributed)

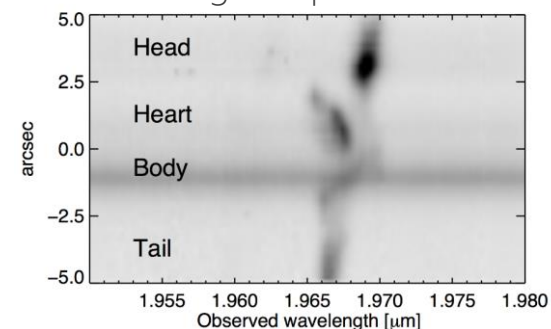
- Older 1 Gyr population → Elevated SF due to *an earlier encounter of the Body and Head*  
Typical timescales between first passage and coalescence (e.g. Johanson+2009)
- Strongest young < 6 Myr starburst in the Head → due to *the on-going interaction*
- > 40 Myr starburst age → second approach of Body and Head happened 50-100 Myr, whereas the Heart appear to be more affected by the on-going merger (shock region)

### 4.1.1 Two or three galaxies

*The origin of Head ?*

- Lower stellar population [Fe/H] abundance of the Head,  
→ Consistent with *the scenario of its separate origin*,  
0.2 dex lower [Fe/H] matches the value expected from mass
- Body systemic velocity is in between that of Head and Tail  
→ A single large progenitor galaxy scenario  
↔ Head appears to be connected to the Body with a faint Pa $\alpha$  velocity structure. Different axis of rotation  
→ *Two-galaxy scenario for Head and Body plausible*
- *Three-galaxy interpretation for the Bird*

Fig. 14.  
Pseudo long-slit spec. of SINFONI



# 4. Discussion

## 4.4.2. Off-nuclear starburst and multiple nuclei

- Bird has a spectacular off-nuclear starburst ↔ ULIRG standard picture (central starburst)
- Toomre  $Q \sim 0.5$  at the Head → SF in the Head is not surprising  
At the Heart  $Q < 1$   
Body has above and below unity value depending on which  $\sigma$  value is used

### *Note*

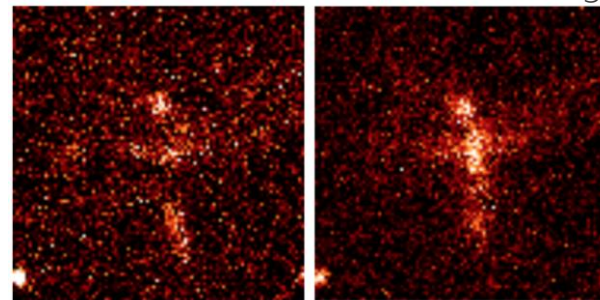
- There may be connection of off-nuclear starbursts to multiple merging (e.g. Borne+2000) and/or the possibility these systems are evidence that ULIRGs typically happen in (compact) groups of galaxies (e.g. Amram+2007)
- Tight groups of galaxies, such as Hickson compact group, may well be candidates (e.g. Borne+2000)

# 5. Bird at high-redshift

HST/B, I band imaged convolved, re-binned, and dimmed to scales at  $z \sim 1-2$

**How is the Bird observed in each wavelength?** Fig. 15. Bird at  $z \sim 1-2$ , based on HST/B(left), I(right)

- Red/infrared (rest V-band & I-band): detect clumpy galaxy (e.g. Shibuya+2016)
- Rest B-band: likely interpret the system as a tight group (Left of Fig. 15)
- Optical (rest-UV): Only see the Head  
→ strongly star-forming compact galaxy



**Would the velocity field be recovered with redshifted  $H\beta$ ,  $H\alpha$ ?**

- Miss the true Body component and its rapidly rotating gas disk
- Head and tidal tails would be interpreted as high-velocity winds  
↔ interacting/merging component

Careful studies of local ULIRGs are needed to interpret observational result of high- $z$  galaxies  
Especially for integrated properties of closely interacting or merging systems